Acta Geotechnica (2016) 11:1103–1109
DOI 10.1007/s11440-015-0421-9

RESEARCH PAPER

Formation and development of salt crusts on soil surfaces

Sheng Dai[1] · **Hosung Shin**[2] · **J. Carlos Santamarina**[3]

Received: 7 July 2014 / Accepted: 17 October 2015 / Published online: 14 December 2015

Abstract The salt concentration gradually increases at the soil free surface when the evaporation rate exceeds the diffusive counter transport. Eventually, salt precipitates and crystals form a porous sodium chloride crust with a porosity of 0.43 ± 0.14. After detaching from soils, the salt crust still experiences water condensation and salt deliquescence at the bottom, brine transport across the crust driven by the humidity gradient, and continued air-side precipitation. This transport mechanism allows salt crust migration away from the soil surface at a rate of 5 μm/h forming salt domes above soil surfaces. The surface characteristics of mineral substrates and the evaporation rate affect the morphology and the crystal size of precipitated salt. In particular, substrate hydrophobicity and low evaporation rate suppress salt spreading.

Keywords Desertification · Efflorescence · Evaporation · Porous media · Salt

✉ Sheng Dai
sheng.dai@ce.gatech.edu

[1] School of Civil and Environmental Engineering, Georgia Institute of Technology, 790 Atlantic Drive, Atlanta, GA 30332, USA

[2] School of Civil and Environmental Engineering, University of Ulsan, Daehak-ro 102, Nam-gu, Ulsan 680-749, South Korea

[3] Earth Science and Engineering, King Abdullah University of Science and Technology, Thuwal 23955-6900, Saudi Arabia

1 Introduction

Salt precipitation plugs pores and generates crystallization pressure that can damage stone, concrete, and ceramics [4, 6, 7, 17, 25–27], affect roads and underground structures [2, 19, 21, 22], and diminish farming land [1, 23]. Climate change may worsen salt precipitation and its impacts [11].

Salt creeping (i.e., crystal development on various substrates) is driven mostly by evaporation. The pioneering work on salt creeping along glass walls concluded that capillarity draws solution upward to the growth front through tiny spaces among crystallites or between the crystallites and the glass wall [37]. It is later suggested that the solution is transported over rather than under the crystallites, given the limited space between the growing crystals and the glass wall [13]. Yet, a recent study using a high-magnification microscope reveals that $K_2Cr_2O_7$ crystal growth is largely determined by the solution transport between the crystallites and the substrate [34].

Recent studies have addressed crystal growth in pores and ensuing damage [3, 9, 28, 31–33], the mechanisms of efflorescence and subflorescence, as well as their emergence as part of transport/evaporation processes [8, 12, 18, 24, 29, 35, 38]. However, the formation and physical properties of salt crusts remain poorly known, primarily due to their thin and fragile characteristics that challenge laboratory experiments [29]. This study explores the formation and migration of the halite (sodium chloride) salt crusts in soils, quantifies the internal structure of the crusts, investigates the effect of the mineral substrate surface conditions on crystallization, and speculates underlying mechanisms of crust migration and detachment from soil surfaces.

2 Experimental studies

We study salt precipitation and crust formation in soils using sand columns saturated with brine (the experimental setup is sketched in Fig. 1). The transparent acrylic cylinder (inner diameter $d_{cyl} = 76.2$ mm, water contact angle 71°) is filled with loosely packed quartzitic sand (Ottawa #20/30 sand, mean grain size $d_{50} = 0.72$ mm, roundness $R_\rho = 0.9$, coefficient of uniformity $C_u = 1.2$, void ratio $e = 0.7$). The sand column is connected to a brine reservoir (NaCl saturated aqueous solution—35.9 g NaCl per 100 g of water at room temperature) to form a free water table inside the specimen about 20 mm below the specimen surface but within the capillary rise (Fig. 1). A high evaporation regime is imposed at the top of the sand surface by continuously blowing low-humidity air (20 °C, relative humidity $RH = \sim 45$ %). Initial evaporation rate is $h = 3.5 \times 10^{-5}$ g/mm^2/s measured using a high-precision balance.

Efflorescence starts closer to the air outlet where the evaporation rate is the highest. Sporadically distributed efflorescence crystallites create more evaporation surface and accelerate water evaporation [29, 35]. Continued crystallizations spread out toward the wall of the acrylic cylinder and gradually cover the entire soil surface forming a crust. This crust continues to evolve and eventually develops into a salt dome that becomes separated from the soil surface and acts as a barrier that slows down evaporation. The salt dome or crust can migrate upwards away from the soil surface apparently "climbing" against the cylinder wall. Differential image processing shows that new salt is continuously precipitating on the crust surface (Fig. 2), yet the crust thickness remains relatively constant after detaching from the soil surface. The upward movement of the salt crust has an average speed of approximately 5 μm/h (for the first 600 h, with a tendency to slow down) under the experimental conditions imposed in this study (Fig. 3). Additional experiments using hydrophobic cylinders (Teflon, water contact angle ~110°) show very limited salt precipitation ahead of the crust on hydrophobic walls, but a detached salt dome still forms.

Salt crust samples are investigated using scanning electron microscopy (SEM). SEM images in Fig. 4 clearly show that sodium chloride salt preferentially precipitates in cubic-shaped crystals that are packed heterogeneously to

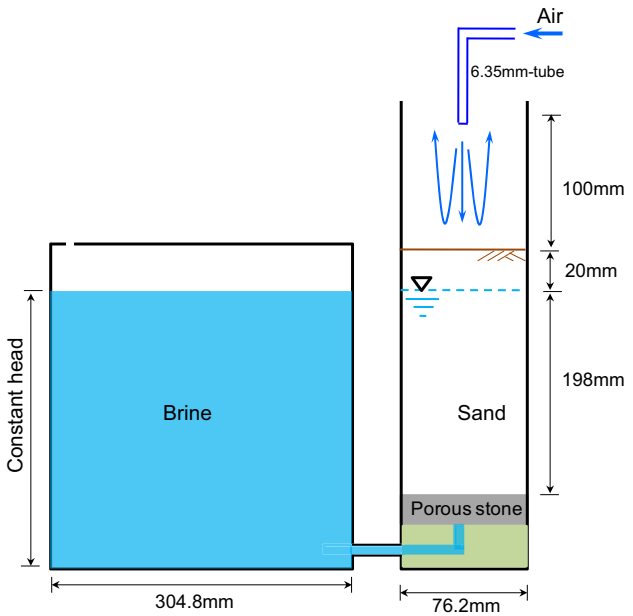

Fig. 1 Experimental configuration. Ottawa #20/30 sand is packed in an acrylic cylinder (inner diameter $d_{cyl} = 76.2$ mm). The bottom of the soil specimen is connected to a constant head brine reservoir (NaCl saturated aqueous solution). Air at $RH \sim 45$ % blows above the specimen to promote evaporation

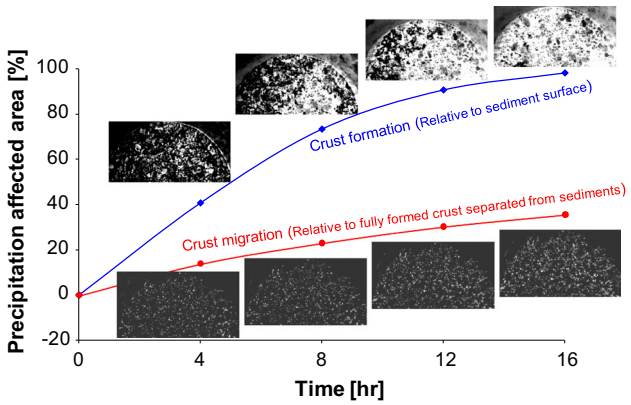

Fig. 2 Salt crust formation and regeneration during migration. *White color* represents newly precipitated salt with respect to the image taken at time zero. Images of crust migration processed here are taken after the crust has separated from the soil surface

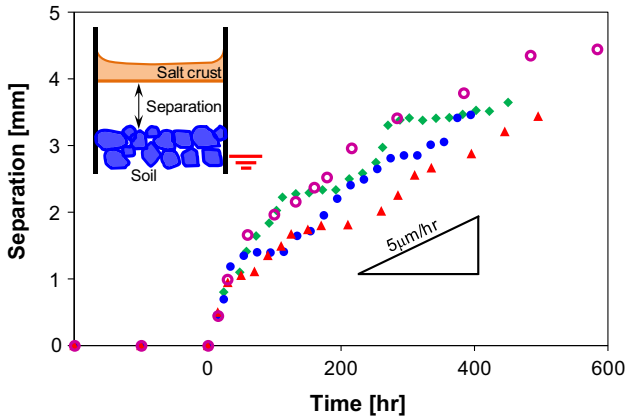

Fig. 3 Salt crust migration away from the sediment surface. As evaporation continues, the salt crust migrates with an average speed of ~5 μm/h during our observation period. Four different symbols here show results of four different runs

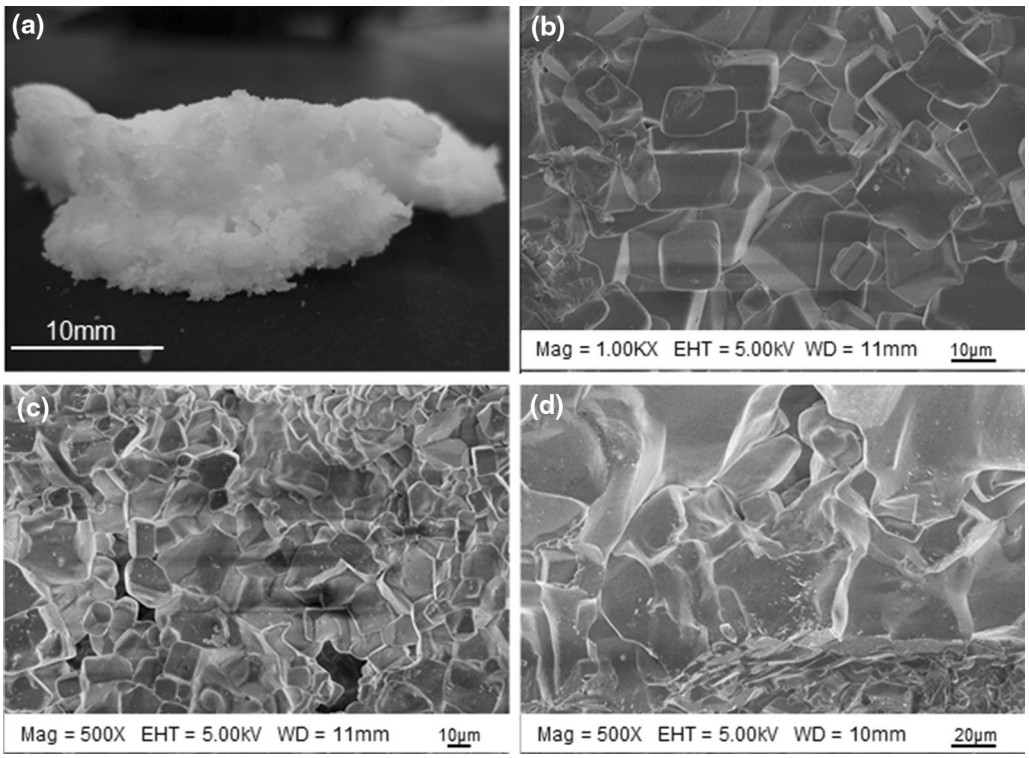

Fig. 4 Porous nature of salt crusts. Photograph (**a**) and scanning electron microscope images (**b**, **c**, **d**) show high porosity and connected micron to submillimeter scale channels. Images (**b**), (**c**), and (**d**) are taken at the *top* (evaporation side), *middle*, and *bottom* side of the crust

form a very porous structure (see also SEM and ESEM images in [5]). This structure is traversed by inter-connected pores and channels that vary in size from micrometers to millimeters. The porosity of this highly porous crust is experimentally determined for the first time using paraffin wax to avoid salt dissolution. The measured porosity of twelve crusts is $n = 0.43 \pm 0.14$ (five measurements for each crust).

3 Analyses and discussion

3.1 Salt crust formation conditions

Evaporation drives the advective transport of solution (i.e., water and hydrated Na^+ and Cl^- ions) to the free soil surface. As water evaporates, ions remain near the free surface. Eventually, salt precipitates on top of the soil specimen (i.e., efflorescence) when the local salt concentration reaches the critical supersaturation (a sufficiently high supersaturation at which crystallization starts to occur). Meanwhile, downward diffusion works against the development of a high salt concentration layer. Thus, crust formation reflects the balance between water evaporation, solution advection, and salt diffusion.

In evaporation-driven advection, the fluid velocity in pores v [m/s] is related to the evaporation rate h [g/mm^2/s] through water mass conservation as a function of the sediment porosity n and the solution mass density ρ_s: $v \approx h/(n\rho_s)$. In general, the evaporation rate decreases with salt concentration [20]; however, early efflorescence may increase the evaporation rate as the exchange surface increases [29]. On the other hand, fully developed salt crusts inhibit water evaporation. Still, evaporation continues through the crust; in fact, evaporation is required to maintain the salt crust or dome, as it would otherwise diffuse away into the saturated bulk solution [14].

The equation for convective-diffusive salt transport in porous media can be written in dimensionless form as [12, 16]:

$$\frac{\partial \Phi}{\partial \tau} = \frac{\partial^2 \Phi}{\partial \zeta^2} - \frac{P_e}{1 - P_e \tau}\left[(\zeta - 1)\frac{\partial \Phi}{\partial \zeta} + \Phi\right], \quad (1)$$

where $\Phi = \rho_{(t,z)}/\rho_0$ is the salt concentration $\rho_{(t,\ z)}$ at time t and location z relative to the far field concentration ρ_0. The dimensionless time $\tau = tD/L^2$ is the elapsed time t normalized by the diffusion constant D and the specimen length L. The dimensionless depth is $\zeta = z/L$. Finally, the Peclet number P_e compares diffusion and advection times $P_e = t_{diff}/t_{adv} = (L^2/D)/(L/v) = vL/D$, where v is the

advection velocity within pores; when $Pe \ll 1$, diffusive transport is more efficient than advection and the ionic concentration remains uniformly distributed throughout the medium; while when $Pe \gg 1$, advection prevails and a concentration accumulation at the evaporating surface occurs. The concentration–depth relations computed with Eq. 1 are shown in Fig. 5a for different Peclet numbers. High evaporation–advection rates, i.e., high Peclet numbers, are needed to increase the salt concentration at the sediment surface in order to cause efflorescence. Salt precipitation may still occur at low Peclet numbers but as subflorescence. Note that in evaporation-driven conditions, the Peclet number can be written as $Pe = hL/(nD\rho_s)$.

Surface evaporation cannot drive advection in systems that are disconnected from a brine reservoir (i.e., no continuous salt solution supply). In this case, the fluid front recedes during evaporation, while salt concentration increases. Diffusion tends to homogenize salt concentration and suppresses salt precipitation once the diffusion rate exceeds the evaporation rate. Therefore, besides low advection rate, low evaporation rate also suppresses crystallization (Fig. 5b).

3.2 Salt crust migration mechanism

Figure 6 schematically illustrates a mechanism proposed herein to explain salt crust migration along the internal wall of acrylic cylinders after detaching from soil surfaces. The detached salt crust hinders evaporation from the soil specimen; thus, the enclosed gap between the soil and the salt crust has a high relative humidity, probably near vapor saturation next to the soil surface. Water molecules from the vapor condense on the bottom of the salt crust forming thin films with properties similar to liquid water [10, 18] and eventually lead to salt deliquescence at the bottom of the crust, where the relative humidity reaches the equilibrium $RH_{eq} = 75$ %. The vapor pressure difference between the bottom ($RH = 75$ %) and the top ($RH = 45$ %) of the salt crust drives the brine solution (from salt deliquescence) across the porous crust to the outer surface, where water molecules evaporate leaving precipitated salt behind. This condensation–deliquescence–transportation–precipitation sequence underlies the upward migration of salt crusts.

The saturated salt solution forms a thin film along walls [15] and sallows solution transport to the crust depending on humidity and the solution concentration [15, 38]. Therefore, the solution film along the cylindrical wall sustains the crust migration. However, the fact that salt crust domes are encountered in natural semiarid environment where there are no walls for transport along solution films suggests that the mechanism of crust migration driven by humidity gradient proposed earlier governs the upward migration of salt crust in nature. Moreover, we observed continuous salt precipitation in the central part of the crust but relatively constant crust thickness once the crust detaches from the soil surface. This observation also favors the self-migration mechanism.

3.3 Effects of substrate surface characteristics

The contact angle and surface tension vary with salt concentration [30]. A complementary set of droplet tests is conducted to investigate the effects of substrate surface on

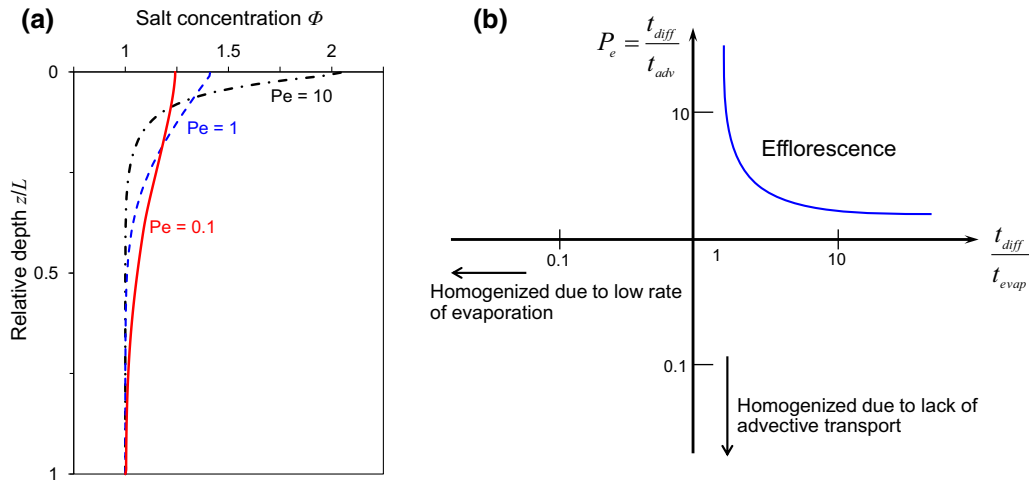

Fig. 5 Efflorescence conditions: dimensionless analyses. **a** Salt concentration profiles at dimensionless time $\tau = 0.1$ as a function of Peclet's number for a system with unlimited supply of solution (i.e., $\Phi = 1$ at $z/L = 1$) during evaporation-driven advection through porous media. When the Peclet number is small (e.g., $Pe = 0.1$), diffusion prevails and lowers salt concentration at the evaporation front. At large Peclet numbers (e.g., $Pe = 10$), salt accumulates at the evaporation front where efflorescence eventually occurs when the salt concentration reaches its critical supersaturation. **b** Efflorescence can be suppressed by slow advection rate in systems connected with continuous brine supply as in (**a**), or slow evaporation rate in closed system disconnected with brine reservoirs or underneath the salt dome

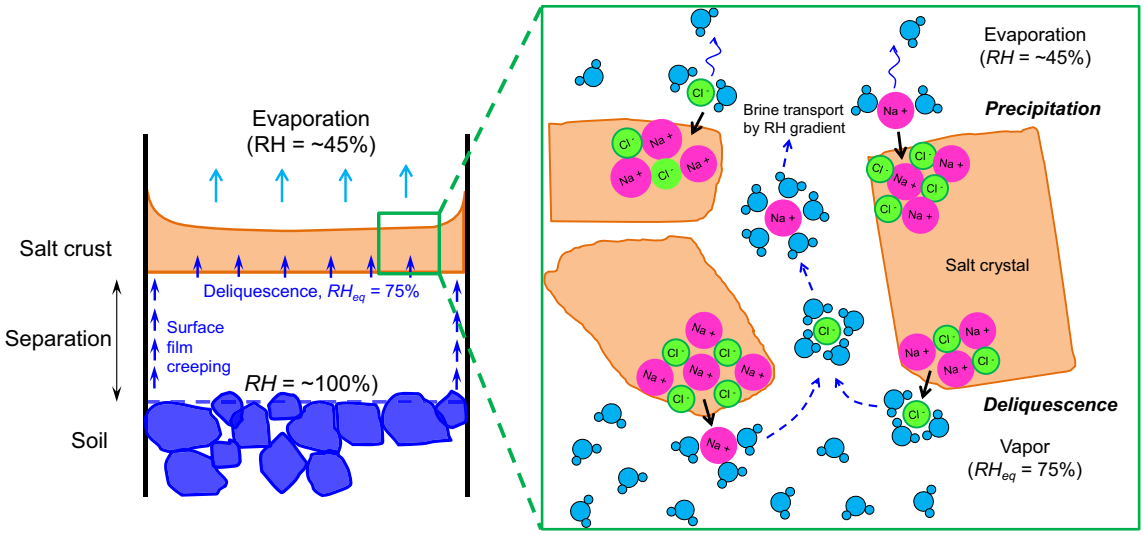

Fig. 6 Hypothesized crust migration mechanism. Vapor condenses and dissolves the salt at the bottom of the crust. The relative humidity gradient across the crust drives ions and water migration through interconnected channels within the crust. Evaporation leaves precipitated salt on the crust upper surface

NaCl salt precipitation characteristics. The size of precipitated salt crystals from aqueous salt droplets (concentration $c = 35$ g/L, similar to that of seawater) increases as the evaporation rate decreases, regardless of substrate surface characteristics (Fig. 7a, see also [36]). Once the salt crust detaches from the bulk solution, the ongoing dissolution–crystallization cycle is limited by saturated solution supply, resulting in lower precipitation rates and crusts with larger crystallites.

We also observed that droplets curl on hydrophobic surfaces (Teflon) but spread out on hydrophilic surfaces (calcite, contact angle 38°) during evaporation; droplets (with identical amount of solution) on hydrophobic surfaces evaporate slower and leave behind larger salt crystals than droplets on hydrophilic calcite (Fig. 7b).

The initial crystallization in the droplet starts near the rim. Further development of the crystals is affected by substrate surface characteristics. The adherence of first few crystallites on the hydrophobic substrate is weakened by the solution transport between the crystallites and the substrate, and the receding of the droplet during evaporation draws the crystals backward (Fig. 7b—left image). However, the first few crystallites tend to adhere to hydrophilic substrate and subsequent evaporation of solution transport over and along the crystallites sustains outward crystallization (Fig. 7b—right image). These two processes are also called "top supplied creeping" and "bottom supplied creeping", respectively [34]. Therefore, besides the suppression of solution protruding the crystallite rims, substrate hydrophobicity also leads to bottom supplied creeping and weakened crystallite adherence to substrates that slows salt migration.

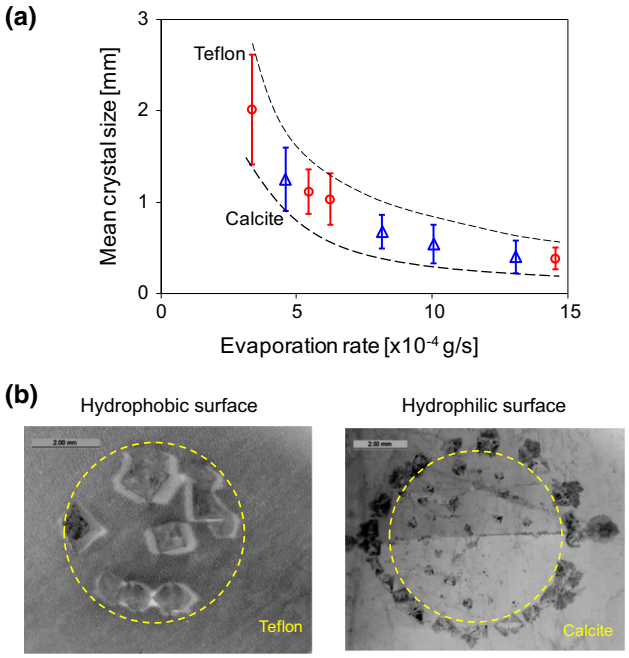

Fig. 7 Evaporation of aqueous salt droplets (initial concentration $c = 35$ g/L similar to seawater). **a** Effect of evaporation rate on precipitated salt crystal size: low evaporation rates result in larger crystals, regardless of substrate characteristics. **b** Mineral substrate surface hydrophobicity affects the morphology of precipitated salt. *Dashed circles* indicate areas initially covered by brine droplets

The effect of the substrate hydrophobicity or hydrophilicity on the topological character of precipitates has been observed in other salts such as $K_2Cr_2O_7$ [34], ammonium chloride [13], potassium nitrate, potassium chloride, and ammonium chloride [13, 38].

4 Conclusions

Salt precipitation, crust formation, and the development of detached domes result from three phenomenological pairs: advection and diffusion, water evaporation and condensation, and dissolution and precipitation.

The rates of diffusion and evaporation combine to restrict conditions for crust formation to $t_{diff}/t_{evap} \gg 1$. Fast brine evaporation leaves behind euhedral cubic-shaped NaCl salt crystals and a highly porous crust structure (porosity 0.43 ± 0.14) with inter-connected micron to submillimeter size pores.

Evaporation pumps brine across the salt crust and supports crust growth. After detaching from the soil surface, the salt crust may still migrate due to water condensation and salt deliquescence at the crust bottom, brine transport across the crust driven by humidity gradient, and continued air-side precipitation. In laterally confined conditions, condensation–deliquescence–transport–evaporation–precipitation can sustain salt crust migration at a speed of 5 μm/h in this study, where solution films along the wall may play a secondary role.

Larger salt crystals form during lower evaporation rates. Mineral surface wetting conditions alter evaporation–precipitation characteristics. In particular, the evaporation rate decreases and larger salt crystals form when droplets rest on hydrophobic surfaces than on hydrophilic surfaces. Substrate hydrophobicity suppresses salt spreading by inhibiting solution protruding ahead of crystallite rims and weakening the crystallite adherence to the substrate. Therefore, salt precipitation can be controlled by engineering mineral surface characteristics and evaporation conditions.

Acknowledgments This work has been supported by the Goizueta Foundation and US Department of Energy. Constructive comments from two anonymous reviewers have greatly improved this manuscript.

References

1. Abrol IP, Yadav JSP, Massoud FI (1988) Salt-affected soils and their management. Food and Agriculture Organization of the United Nations, Rome
2. Alonso EE, Olivella S (2008) Modelling tunnel performance in expansive gypsum claystone. In: International association for computer methods and advances in geomechanics (IACMAG), 891–910
3. Angeli M, Bigas J-P, Benavente D, Menéndez B, Hébert R, David C (2007) Salt crystallization in pores: quantification and estimation of damage. Environ Geol 52:205–213
4. Benavente D, Cueto N, Martínez-Martínez J, Del Cura MG, Cañaveras J (2007) The influence of petrophysical properties on the salt weathering of porous building rocks. Environ Geol 52:215–224
5. Benavente D, del Cura M, Garcıa-Guinea J, Sánchez-Moral S, Ordóñez S (2004) Role of pore structure in salt crystallisation in unsaturated porous stone. J Cryst Growth 260:532–544
6. Cardell C, Rivas T, Mosquera M, Birginie J, Moropoulou A, Prieto B, Silva B, Van Grieken R (2003) Patterns of damage in igneous and sedimentary rocks under conditions simulating sea-salt weathering. Earth Surf Process Landf 28:1–14
7. Chatterji S, Jensen AD (1989) Efflorescence and breakdown of building materials. Nordic Concr Res 8:56–61
8. Eloukabi H, Sghaier N, Ben Nasrallah S, Prat M (2013) Experimental study of the effect of sodium chloride on drying of porous media: the crusty–patchy efflorescence transition. Int J Heat Mass Transf 56:80–93
9. Espinosa-Marzal RM, Scherer GW (2010) Advances in understanding damage by salt crystallization. Acc Chem Res 43:897–905
10. Foster MC, Ewing GE (2000) Adsorption of water on the NaCl(001) surface. II. An infrared study at ambient temperatures. J Chem Phys 112:6817–6826
11. Goudie A, Viles HA (1997) Salt weathering hazards. Wiley, Chichester
12. Guglielmini L, Gontcharov A, Aldykiewicz JAJ, Stone HA (2008) Drying of salt solutions in porous materials: intermediate-time dynamics and efflorescence. Phys Fluids 20:077101–077107
13. Hazlehurst T Jr, Martin H, Brewer L (1936) The creeping of saturated salt solutions. J Phys Chem 40:439–452
14. Hird R, Bolton M (2014) Upward migration of sodium chloride by crystallization on non-porous surfaces. Phil Mag 94:78–91
15. Huang B-J, Huang J-C (1976) Creeping-film phenomenon of potassium chloride solution. Nature 261:36–38
16. Huinink HP, Pel L, Michels MAJ (2002) How ions distribute in a drying porous medium: a simple model. Phys Fluids 14:1389–1395
17. Mokni N, Olivella S, Alonso EE (2010) Swelling in clayey soils induced by the presence of salt crystals. Appl Clay Sci 47:105–112
18. Nachshon U, Shahraeeni E, Or D, Dragila M, Weisbrod N (2011) Infrared thermography of evaporative fluxes and dynamics of salt deposition on heterogeneous porous surfaces. Water Resources Research 47, n/a–n/a
19. Netterberg F, Loudon P (1980) Simulation of salt damage to roads with laboratory model experiments. In: Proceedings of the seventh regional conference for Africa on soil mechanics and foundation engineering, Accra, June 1980, p. 7
20. Norouzi Rad M, Shokri N (2012) Nonlinear effects of salt concentrations on evaporation from porous media. Geophys Res Lett 39:L04403
21. Obika B, Freer-Hewish R, Fookes P (1989) Soluble salt damage to thin bituminous road and runway surfaces. Q J Eng GeolHydrogeol 22:59–73
22. Oldecop L, Alonso E (2012) Modelling the degradation and swelling of clayey rocks bearing calcium-sulphate. Int J Rock Mech Min Sci 54:90–102
23. Rengasamy P (2010) Soil processes affecting crop production in salt-affected soils. Funct Plant Biol 37:613–620
24. Rodriguez-Navarro C, Doehne E (1999) Salt weathering: influence of evaporation rate, supersaturation and crystallization pattern. Earth Surf Process Landf 24:191–209
25. Sayward JM (1984) Salt action on concrete. U.S. army cold regions research and engineering laboratory, Special Rpt. 84–25, p. 76
26. Scherer GW (2004) Stress from crystallization of salt. Cem Concr Res 34:1613–1624
27. Scherer GW, Flatt R, Wheeler G (2001) Materials science research for the conservation of sculpture and monuments. MRS Bull 26:44–50
28. Schiro M, Ruiz-Agudo E, Rodriguez-Navarro C (2012) Damage mechanisms of porous materials due to in-pore salt crystallization. Phys Rev Lett 109:265503

29. Sghaier N, Prat M (2009) Effect of efflorescence formation on drying kinetics of porous media. Transp Porous Media 80:441–454
30. Sghaier N, Prat M, Ben Nasrallah S (2006) On the influence of sodium chloride concentration on equilibrium contact angle. Chem Eng J 122:47–53
31. Shahidzadeh-Bonn N, Desarnaud J, Bertrand F, Chateau X, Bonn D (2010) Damage in porous media due to salt crystallization. Phys Rev E 81:066110
32. Steiger M (2005) Crystal growth in porous materials—I: the crystallization pressure of large crystals. J Cryst Growth 282:455–469
33. Steiger M (2005) Crystal growth in porous materials—II: influence of crystal size on the crystallization pressure. J Cryst Growth 282:470–481
34. van Enckevort WJ, Los JH (2013) On the creeping of saturated salt solutions. Cryst Growth Des 13:1838–1848
35. Veran-Tissoires S, Marcoux M, Prat M (2012) Discrete salt crystallization at the surface of a porous medium. Phys Rev Lett 108:054502
36. Vrhunec A, Kolenc A, Teslic D, Livk I, Pohar C (1999) Crystal size distribution in batch sodium perborate precipitation. Acta Chim Slov 46:543–554
37. Washburn ER (1927) The creeping of solutions. J Phys Chem 31:1246–1248
38. Zhang H, Wu Z, Francis LF (2009) Formation of salt crystal whiskers on porous nanoparticle coatings. Langmuir 26:2847–2856